

SYNTHESIS AND CHARACTERIZATIONS OF NICKEL OXIDE NANOPARTICLES BY PVA MATRIX METHOD

K. Siddique*

S. Karmakar*

Abstract:

NiO nanoparticles were prepared by PVA matrix method with an average grain size of 25-75 nm. The prepared NiO nanoparticles were characterized by XRD (X-ray diffraction), XRF (X-ray fluorescence), TEM (Transmission Electron Microscopy), FT-IR Spectroscopy and VSM. It is found that, calcination temperature effects widely on the grain size and other properties of NiO nanocrystals. The magnetic properties of these particles show significant variation such as increase in saturation magnetization, coercivity etc. with rise in calcination temperatures. But the band gap of the NiO nanoparticles decreases with the increase in calcinations temperatures.

Keyword: XRD, TEM, M-H Curve, FT-IR, Metal Oxides etc.

* Department of Instrumentation & USIC, Gauhati University, Guwahati -781014, India

Introduction:

Like other transition metal oxides viz. MnO, FeO and CoO, NiO has attracted much attention in recent years for its catalytic, electronic and magnetic properties [1-3]. The Nano-structure is expected to possess many exciting properties than those of bulk NiO powder [4-7]. Nanocrystalline NiO particles are much more effective catalysts than commercial NiO powder for catalytic reduction of carbon dioxide to methanol [8-10]. Among all these oxides, NiO exhibits many nanostructures: nanosheet, nanoring, nanorods, ordered hexagonal mesostructures, and hollow sphere [11-13]. NiO is an important inorganic and in nature it occurs as mineral besenite having cubic rock salt (NaCl type) structure with $a = 4.915 \text{ \AA}$ and also it is available in two different forms: pale apple green or jet black depending upon the stoichiometry. Nanocrystalline NiO has found application in electrochromic applications, electrochromic coatings, P-type transparent conducting films, electrochemical supercapacitor, -ve electrode of lithium ion batteries, catalyst and antiferromagnetic materials.

A number of preparation methods have been reported in literature, namely, chemical liquid precipitation method, laser spray pyrolysis method, physical vapour method, Sol-gel method, sputtering, thermal decomposition method and many more. In this paper, we have reported synthesis of Nanocrystalline NiO using chemical liquid precipitation method in polyvinyl alcohol.

Experimental details:

0.1 M 10 ml water solution of Nickel nitrate hexahydrate $[\text{Ni}(\text{NO}_3)_2 \cdot 6\text{H}_2\text{O}]$ (A) was prepared. 10% wt. solution of Polyvinyl alcohol in water (B) was prepared under constant stirring at 80°C temperature. Solution (A) was then added to solution (B) at room temperature at constant stirring for 15 min. The alkalinity of the reaction mixture was increased by adding drop by drop aqueous solution of 10 ml of NaOH (0.75 M) and a gel was produced and dried. Finally the dried gel was calcined at different temperatures in static air for different times. The black/brown powder obtained after calcination was washed first with hot water and then with cold water for several times and finally dried in an oven at 60°C for overnight.

In the present paper we studied the size, shape magnetic and morphological properties with the variation of calcination temperatures. We calcined the metal dispersed PVA gel at four different temperatures keeping all other conditions constant.

All the chemicals used in this work are commercial grade, purchased from commercial market and used without further purification. Thus $[\text{Ni}(\text{NO}_3)_2 \cdot 6\text{H}_2\text{O}]$ and sodium hydroxide (NaOH) were purchased from E. Merck (India). Polyvinyl alcohol (PVA Mol. Wt. =115000) was obtained from Loba Chemical (India).

Results

X- Ray diffraction (XRD):

The XRD patterns of the prepared samples with different increasing calcination temperatures viz. 400°C , 500°C , 600°C , 700°C respectively are obtained from Philips make (X'PERT PRO) diffractometer using CuK radiation (40 kV, 30 mA) and are shown in Fig.1. The diffractometer is calibrated with the standard silicon sample. The patterns show that the compound is polycrystalline in nature and the NiO (Hanawalt et. Al.,1938) phase is present. It is found that the crystals are formed in cubic system with lattice parameters $a=b=c=4.168 \text{ \AA}$ which is in good agreement with those found (4.171 Å) for the standard (ICDD No. 01-1239). The peaks seem to be appreciably broad which indicate that the crystalline size of the NiO is in nano range. It has been found that as the calcinations temperature is increased, peaks are become more and more sharp with reduced broadening, which indicate the increase in grain size with increasing temperatures. Peaks are obtained at 37.473° , 43.510° , 63.261° , 75.446° , and 79.947° 2θ values which are indexed as (111), (200), (220), (311) and (222) respectively.

The particle sizes were calculated from the prominent peaks using Scherrer formula (14)

$$D = \frac{0.89\lambda}{\beta \cos \Theta} \quad (1)$$

Where λ is the wavelength of X-ray used, β is Full width at half maxima (FWHM) in radian and Θ is the half of the Bragg's diffraction angle.

Table.1 shows the variation of particle size of NiO Nanoparticle with the calcination temperatures. It is seen that as the calcination temperature increased, the particle size is also gradually increased which is due to the increase in crystallinity at high temperatures. It is interesting to see that at low temperatures (400°C, 500° C 600°c and 700°C), two peaks of Ni are also present in the diffractograms (Fig. 1). This is due to the fact that a small fraction of Nickel is not oxidised showing low intensity peaks of nickel ion at 44.49° and 51.87°. But as the temperature is increased these Nickel ions get oxidized and the corresponding peaks were vanished at 700°c calcinations temperature.

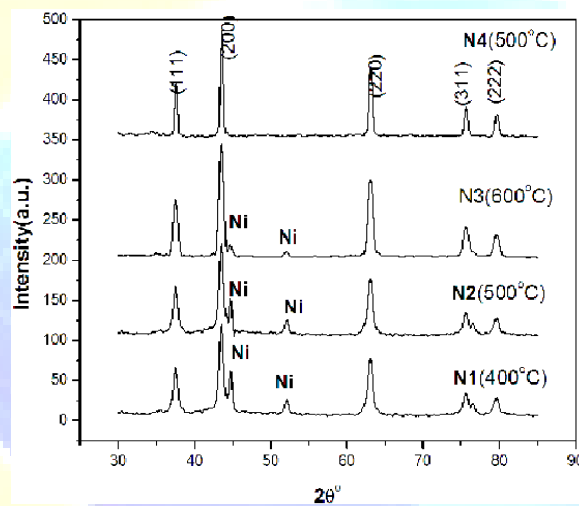


Fig.1 XRD patterns of NiO Nanocrystalline particles at different annealing temperatures

400°C(N1), 500°C(N2), 600°C(N3) & 700°C(N4)

1.2. Lattice constant:

The lattice parameter ‘a’ for cubic structure is determined using the following

$$a = d (h^2+k^2+l^2)^{1/2} \quad (2)$$

where ‘d’ is the perpendicular distance between the two consecutive planes in the atomic lattice and the (h k l) are the miller indices. The lattice constants are calculated from the

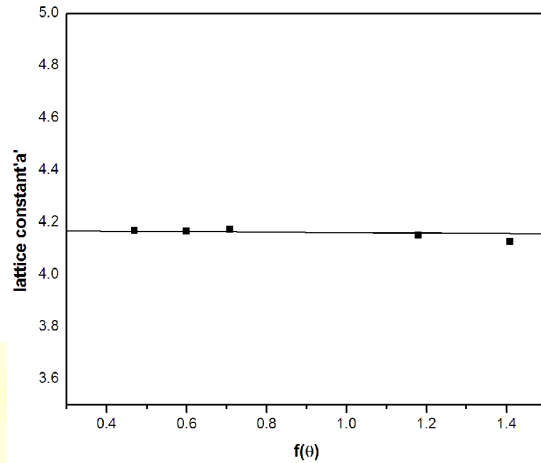


Fig.2 Nelson –Riley plot for lattice constant.

peak of high intensities. There is a slight deviation of lattice parameter from the standard value due to the divergence of X-ray beam from the refraction and absorption of X-ray by the specimens etc. which involve a numbers of systematic errors in the measurement of ‘ Θ ’ and ‘ d ’ values. Therefore the corrected value of lattice constants are estimated from the Nelson-Riley plot [17] which is plotted between the calculated ‘ a ’ for different planes and the error function

$$f(\theta) = \frac{1}{2} \left[\frac{\cos^2 \theta}{\sin \theta} + \frac{\cos^2 \theta}{\theta} \right] \quad (3)$$

Extrapolating the graph, the point of intersection ($\Theta=90^\circ$) with the y-axis is found out to be 4.16 Å gives the corrected values lattice constant ‘ a ’ as shown in fig 2.

1.3. Dislocation density(δ) and microstrain(ϵ):

The dislocation density (δ) is calculated from the Williamsons and smallman’s formula,

$$\delta = \frac{n}{D^2} \quad (4)$$

Where ‘ n ’ is a factor which is equal to unity giving minimum dislocation density and ‘ D ’ is the average grain size. The calculated dislocation density is shown in Table 3.

Micro strain(ϵ) is obtained using the relation[16-17]

$$\varepsilon = \frac{\beta \cos \theta}{4} \quad (5)$$

Where ‘ β ’ is the full width at half maximum intensity and θ is the half of Bragg’s angle. The calculated values are shown in the Table 3. The values of microstrain and dislocation density decrease with the increase in calcination temperatures.

Microstrain calculated for all the sample was found to be of the order of 10^{-3} because of that the W-H plot become parallel to the X-axis [16-17].

Table.1 Particle size of NiO nanoparticle at different annealing temperatures:

| Calcination temperature °C | Average crystalline size nm | Dislocation density $\times 10^{15}$ | Microstrain $\times 10^{-3}$ |
|-------------------------------|-----------------------------|-----------------------------------------|---------------------------------|
| 400 | 31 | 1.040 | 3.243 |
| 500 | 27 | 1.371 | 2.926 |
| 600 | 39 | 0.657 | 2.005 |
| 700 | 62 | 0.2601 | 1.472 |

3. TEM:

The HRTEM image (Fig. 4a) of the synthesized nanoparticles are taken in a Jeol JEM 2100 200Kv shows that the particles are uniformly cubic in shape and but the size distribution is non-uniform. It is also found that particle size increases with the increase in calcination temperatures. It is expected that higher calcination temperature will increase the particle size due to sintering of the small particles into larger particles. This type of aggregation occurs at higher temperature in order to minimize the high surface energy. The average crystallite size of the NiO nano particles

obtained by TEM analysis are compared with those obtained from XRD analysis (Table 2.). The interplanar spacing (d-value) also obtained from TEM analysis which was found to be the order of 0.200 nm. The d-value calculated from XRD is found to be the order of 0.207 nm from the indexed plane (2 0 0). Both d-values are in the same range which is expected. Selected area diffraction pattern (SEAD) shows the polycrystalline nature of the prepared NiO nanoparticle which is shown in the inset of Fig4b.

Table.2

| Calcination temperature | Particle Size from XRD(nm) | Particle Size from TEM(nm) |
|-------------------------|----------------------------|----------------------------|
| 400 | 31 | 32 |
| 500 | 27 | 28 |
| 600 | 39 | 40 |
| 700 | 62 | 75 |

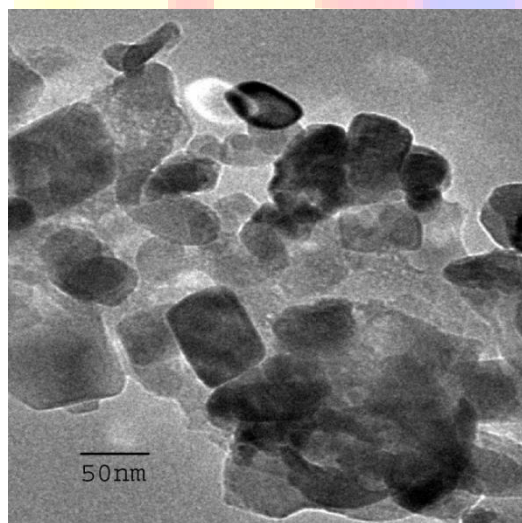


Fig.4(a)

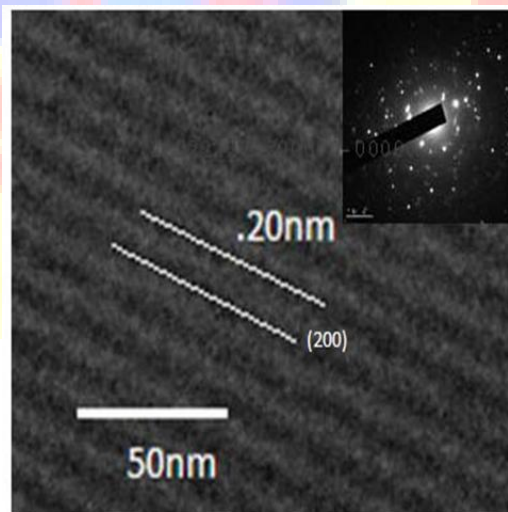


Fig.4(b)

Fig.4 TEM Images of sample N4 (a) particle size (b) lattice plane & SEAD

5.FT-IR:

Broad absorption peak at 3430cm^{-1} is obtained due to O-H stretching vibrations of moisture . The sharp peak at 2673 cm^{-1} is due atmospheric $\text{O}=\text{C}=\text{O}$ Stretching of air.The strong band at 460cm^{-1} indicates the presence of O- Ni-O bond.

Magnetic properties:

Fig.7 shows the typical magnetization curves and hysteresis loops for the synthesized metal oxide nanoparticles. The observed value of saturation magnetization (M_S) for N4 is 58.9×10^{-3} emu/g which is much lower than that of the reported M_S value of the multi-domain bulk NiO. The decrease in M_S occurs due to decrease in magnetic moment which is in turn decreases at low particle size [18]. This can be attributed to the surface contribution, surface defects, stoichiometry deviation [19]. The saturation magnetization values for the samples N1, N2 and N3 are found to be 17×10^3 emu/g 45×10^{-3} emu and 54.7×10^{-3} emu/g respectively which are much lower than those values obtained theoretically for the bulk. Value of coercivity for N1 , N2, N3 and N4 are 167.04 G, 141G, 218G and 285G respectively. This anomalous magnetic behaviour may be due to different crystal anisotropy and shape anisotropy [23]. high coercivity shows the well magnetic behavior.

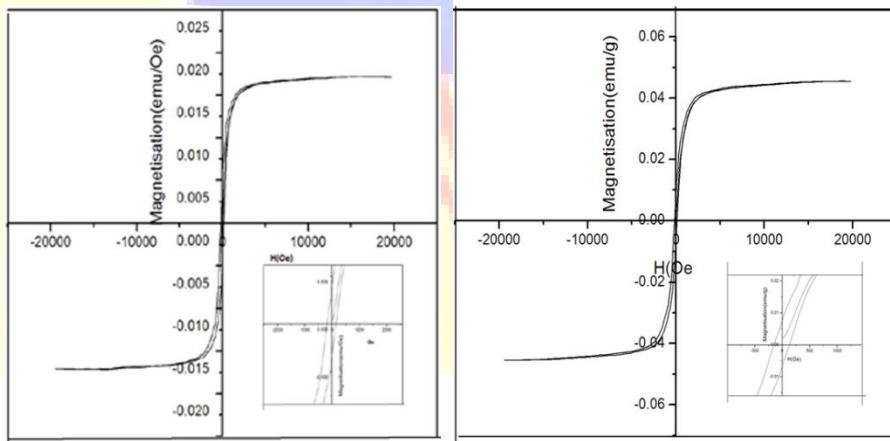


Fig.7(a)

Fig.7(b)

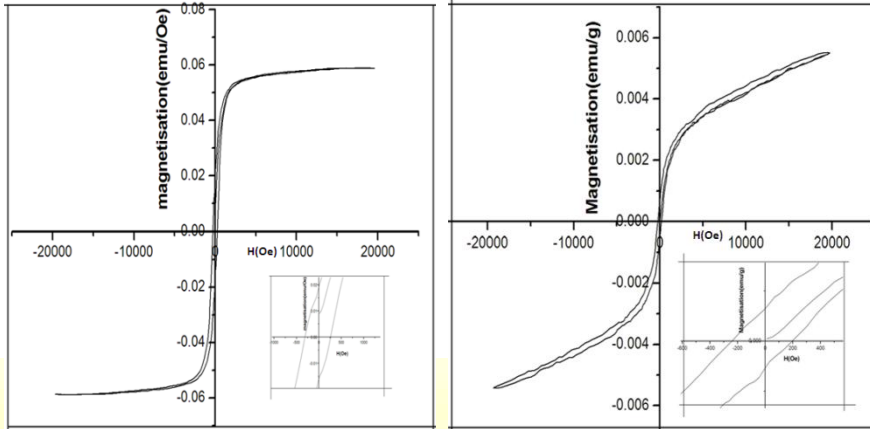


Fig.7(c)

fig.7(d)

Fig. 9 M-H Curve for NiO at different calcinations temperature (a) 400°C (b) 500°C (c) 600°C and (d) 700°C

Conclusion:

The XRD Spectra shows the nanocrystalline pattern of NiO. The grain size varies from 25 nm to 75nm with the varying calcination temperature. But the variation of band gap with the variation of calcination temperatures viz. 400°, 500°, 600° 700°C are found to be increased from 4.91 eV to 4.95 eV. The XRD, XRF and FT-IR spectra show the well formation of NiO particles. From the Study of M-H Curve it has been found that Saturation magnetic field increases from 17 X10³, 45X10⁻³, 54.7X10⁻³ and 58.9 X 10⁻³ and coercivity varies from are 167.04 G, 141G, 218G and 285G with the calcinations temperature increases from 400°, 500°, 600° 700°C respectively.

Reference:

- 1.C.L. Cabrne, K.J. Klabunde, J. Mol.Catal. A, Chem. 194(2003)227
- 2.V.Biju, M. Abdul Khadar, Mater. Sci. Eng.:A304-306(2001)814
3. Y.Ichianagi, N. Wakabayashi, J. Yamajaki, S. Yamada, Y. Kimishima, E. Komatsu, H. Tajima, PhysicaB329-333(2003-2001)814
4. L.Wu, Y.Wu, H. Wei, Y.Shi, C.Hu, Mater. Lett. 58(2004)2700
5. C.L. Cabrne, K.J. Klabunde, J. Mol.Catal. A, Chem. 194(2003)227
6. D. L. Tao, F.Weil Mater. Lett. 58(2004)3266
7. V.Biju, M. Abdul Khadar , Spectrochim. Acta partA 59(2003)121
8. J. bahadur, D. Sen S. Mazumdar, S. Ramanathan, j. solid State Chemistry181(2008)1227-1235
- 9.H. Sato , T. minami, S. Takata, T. Yamada, Thin solid film 226(1993)27
10. B.L.Cushing kolesnichenko, C.J. O'connor, chemical review104(2004)1227-1235
- 11.H.J. Lui, T. Y. Peng, D.E.Zhao, K.Dai, Z.H.Peng, matter.Chem. Phys. 87(2004)81
- 12.Z.H.Liang, Y.J.Zhu, X.L.Hu, J. Phys. Chem. B108(2004)3488
13. D.B. Wang, C.X. Song, Z.S.Hu, X.Fu, J.phys Chem.B 109(2005)1125
14. B.D. Cullity, element of X-ray diffraction , Addison -Wesley, Reading massachusetts356(1979)
- 15.Lifshim, (1999), X-ray Chracterization of materials, Wiley New york, p 37
- 16.Girija.K, Thirumalairajan. S, Mohan. S.M, Chandrasekaran. J. Chalcogenide 351-357(2009)6
- 17 B.D. Cullity, element of X-ray diffraction , Addison -Wesley, Reading massachusetts327-335(1979)
- 18 Mounien N, Pileni M. P, *Langmuir* 13 (1997) 3927
- 19Goya G F, Berquo M, Fonseca T S, *Appl Phys* 94 (2003) 3520
- 20Zhang D, Zhang X, Ni X, Song J, Zheng H G, *Cryst Growth Des* 10 (2007) 2117.